Specifics of substrate-mediated photo-induced chemical processes on supported nm-sized metal particles

2004 J. Phys.: Condens. Matter 16 7131

(http://iopscience.iop.org/0953-8984/16/39/044)

INSTITUTE OF PHYSICS PUBLISHING JOURNAL OF PHYSICS: CONDENSED MATTER

J. Phys.: Condens. Matter **16** (2004) 7131–7141 PII: S0953-8984(04)81458-9

Specifics of substrate-mediated photo-induced chemical processes on supported nm-sized metal particles

Vladimir P Zhdanov[1,2] **and Bengt Kasemo**[1]

[1] Department of Applied Physics, Chalmers University of Technology, S-412 96 Göteborg, Sweden
[2] Boreskov Institute of Catalysis, Russian Academy of Sciences, Novosibirsk 630090, Russia

E-mail: zhdanov@catalysis.nsk.su

Received 1 June 2004
Published 17 September 2004
Online at stacks.iop.org/JPhysCM/16/7131
doi:10.1088/0953-8984/16/39/044

Abstract

Substrate-mediated mechanism of photochemical reactions on metals includes direct and/or plasmon-related excitation of electron–hole pairs in the bulk by photons and subsequent chemical transformation due to interaction of excited (hot) electrons (or holes) with the adsorbate. In nm-sized metal particles, the excited electrons are confined. We show in detail that this factor is beneficial for photochemistry under low-intensity steady-state conditions (linear regime) and also during intensive sub-ps laser pulses (non-linear regime). In both cases, the confinement may increase the contribution of secondary hot electrons to the photochemical conversion. In addition, in the non-linear regime the decrease of electron temperature after heating may be much slower than that on the surfaces of bulk samples and accordingly photochemical reactions may be more probable.

1. Introduction

During the past two decades, photochemistry on metal surfaces has been rapidly developing [1–5]. The available experimental and theoretical studies have primarily been focused on processes occurring on single-crystal surfaces. In applications, photochemical reactions are likely to run on structurally more complex systems. In analogy with conventional catalysis, the most promising candidates are supported metal (or non-metal) particles with a size of 1–10 nm (larger particles or layered substrates may be useful as well [6]). Recent examples of photo-induced processes on catalysts of the latter category include methane and NO desorption and CO adsorption-site exchange on Pd/Al_2O_3 [7–9] (for a few other examples, including surface complexation with organic molecules, dye-capped metal nanoclusters, and photo-induced energy- and electron-transfer processes between excited sensitizer and metal nanocore, see [10]). Some of the benefits of nm-sized metal particles are obvious (e.g. high

surface area, new sites for adsorption and reaction, and the possibilities to tune optical properties by changing the size and shape of particles and the distance between particles [11, 12]). Other benefits (or shortcomings) are however less clear, due to the lack of a deeper understanding of the details of photochemical processes in this case. The goal of the present paper is to scrutinize the specifics of *substrate-mediated* photo-induced chemical processes (SMPCP) on nm-sized metal particles in order to clarify potential advantages here compared to surfaces of bulk samples (in the discussion below the latter are taken to be a single-crystal surface).

In adsorbed overlayers on a single-crystal surface [1, 2, 5], SMPCP most commonly occur via (i) optical excitation of primary electron–hole pairs in the bulk, (ii) migration of these excitations to the surface, accompanied by excitation of secondary electron–hole pairs or phonons, and (iii) inelastic scattering or trapping of hot electrons (or holes) from or to the adsorbate, resulting in chemical transformation, i.e. bond breaking and/or bond formation (to be specific, we discuss below the chemical processes related to scattering or trapping of electrons). This general scheme allows two complementary scenarios. The first one includes initiation of all the elementary events by a single photon. The second one implies heating of electrons near the surface and multiple inelastic electron scattering from the adsorbate. At low light intensities, SMPCP may only occur via the first scenario. The second scenario can be realized, e.g. by using intensive sub-ps pulses of visible light. In the latter case, SMPCP occurs via scenario 1 in the very beginning but then rapidly turns to scenario 2. Below, we discuss these scenarios in sections 2 and 3, respectively. In both sections, we first briefly recall what is going on in the case of SMPCP on a flat surface, and then show what one can expect for SMPCP on nm-sized metal particles.

2. Scenario 1

According to the first scenario, the cross section of SMPCP on a single-crystal surface can phenomenologically be represented as

$$\sigma(\omega) \propto \int_0^{\hbar\omega} \mathcal{P}(E)\mathcal{F}(\omega, E)\,\mathrm{d}E, \tag{1}$$

where $\mathcal{F}(\omega, \mathcal{E})$ is the photon-initiated electron flux towards the surface, $\mathcal{P}(\mathcal{E})$ the reaction probability due to inelastic scattering or trapping of a single hot electron, and E and $\hbar\omega$ are the electron and photon energies, respectively.

The electron flux is assumed to be formed by primary electrons, generated by photons, and a cascade of secondary electrons. The first generation of secondary hot carriers (electrons and holes) is due to electron–hole pair excitation by primary carriers. The second generation of hot carriers is due to electron–hole pair excitation by the first generation, etc. The interaction between hot carriers is neglected. The interaction with phonons is usually neglected as well, as long as the electron energy is not too low. Each elementary chemical event is considered to result from inelastic scattering or trapping of a single electron.

To calculate $\mathcal{F}(\omega, E)$ in equation (1), it should be taken into account that the concentration of primary hot carriers created at a distance z from the surface is proportional to $A\alpha \exp(-\alpha z)$, where A is the substrate absorbance and α the optical absorption coefficient. To describe the fate of these carriers, one needs to specify their energy distribution and energy-dependent mean free path. In our discussion, we will mainly consider noble metals because compared to other metals, in analogy with conventional catalysis, they are expected to be usually superior in photocatalysis. In this case, absorption of light with $\hbar\omega \geqslant 4\,\mathrm{eV}$ is well known to occur primarily via transitions from the d bands into the sp conduction bands. The free-electron

contribution dominates at $\hbar\omega \leqslant 2$ eV. Between these energies, the situation is metal-specific. For the d $\rightarrow$ sp transitions, the energy distribution of primary electrons strongly depends on the position and width of the d band. In the free-electron case, one can make the reasonable assumption that the energy distribution of primary electrons is uniform,

$$f_0(E) = 1/(\hbar\omega). \tag{2}$$

The secondary electrons and holes are mainly generated in the sp conduction band. According to the free-electron model the properties of electron and holes near the Fermi energy are nearly identical [13] (for more recent treatments, see [14, 15]). In particular, the electron or hole energy distribution after the creation of a new electron–hole pair can be represented as

$$\varphi(E, E') = 2(E - E')/E^2, \tag{3}$$

where E and E' are the energies before and after scattering. The inverse mean free path of electron and holes is given by

$$\beta(E) = \beta_0[(E - E_F)/E_F]^2, \tag{4}$$

where β_0 is the parameter determined by the free-electron density of the metal.

To use equation (1), one also needs to specify $\mathcal{P}(E)$. The simplest dependence convenient for our discussion is given by

$$\mathcal{P}(E) \propto \delta(E - E_0), \tag{5}$$

where E_0 is the resonant energy corresponding to attachment of a hot electron to the adsorbate [usually a LUMO (electrons) or HOMO (holes) orbital], and $\delta(E)$ is the delta function (in principle, one can introduce a finite width of the resonance, but for our present goals it is not necessary).

Assuming, for example, that the SMPCP is mainly due to primary electrons and using the 1D model for propagation of these electrons, one has

$$\mathcal{F}(E) \propto A\alpha \int_0^\infty \exp\{-[\alpha + \beta(E)]z\}\,\mathrm{d}z = A\alpha/[\alpha + \beta(E)]. \tag{6}$$

Substituting equations (5) and (6) into (1) yields

$$\sigma \propto A\alpha/[\alpha + \beta(E_0)]. \tag{7}$$

Equation (7) was first presented by Ertl and co-workers in their seminal treatment [16] of photo-induced dissociation of O_2 on Pd(111) (another example is K desorption from graphite [17]). The contribution of secondary electrons to SMPCP on a single-crystal surface was analysed in [18–21]. A general conclusion drawn on the basis of the calculations presented there is that this contribution is important if E_0 is appreciably lower than $\hbar\omega$. Concerning the details of calculations in [18–21], it is appropriate to note that the work [18] is based on the assumptions that (i) after excitation of an electron–hole pair by an electron the energy distribution of two electrons is flat [$\varphi(E, E') = 1/E$] and (ii) generation of secondary electrons due to excitation of electron–hole pairs by holes is negligible. Both these assumptions should be corrected (see equation (3) above and equation (11) below). For this reason, the electron flux distribution $\mathcal{F}(\omega, E)$, obtained in [18] and used in [21], cannot be employed in applications. In [20], assumption (i) was dropped but assumption (ii) was still held. Thus, the electron-flux distribution reported there is also not quite correct. None of these shortcomings are present in [19], but the treatment presented there only takes into account primary electrons and the first generation of secondary electrons.

The size of the metal particles under consideration is smaller than or comparable to $1/\alpha$ and $1/\beta$. This means that the elementary events occurring with participation of electrons and holes should in this case be discussed in terms of rate constants instead of such terms as 'optical absorption coefficient' and/or 'mean free path'. Specifically, equation (1) has to be rewritten as

$$\sigma(\omega) \propto A \int_0^{\hbar\omega} [p(E) f(\omega, E)/r(E)]\, \mathrm{d}E, \tag{8}$$

where $f(\omega, E)$ is the distribution of electrons generated inside the metal particle by a single absorbed photon, $p(E)$ the rate constant corresponding to initiation of the desired process due to interaction of an electron with an adsorbed species and $r(E)$ the electron energy relaxation rate constant. Using equation (8), we imply $r(E) \gg p(E)$.

The rate constant p increases with the increasing area of the metal particle (due to the increase of the available number of adsorbed species) but decreases with the increasing volume of the metal particle (because an excited electron is distributed over the whole particle). Due to the combination of these factors, one gets $p \propto 1/R$, where R is the metal-particle radius. Adopting in addition equation (5) in order to describe the energy dependence of p, we have $p(E) \propto (1/R)\delta(E - E_0)$. Substituting this expression into equation (8) yields

$$\sigma \propto A f(\omega, E_0)/[r(E_0)R]. \tag{9}$$

Compared to a single-crystal surface, the absorbance of nm-sized particles may be somewhat reduced due to their small size ($R < 1/\alpha$). This can however be compensated by the factor $1/R$ in equation (9). In addition, the absorbance of such particles can actually be appreciably enhanced due to their unique optical properties, for example, due to excitation of nanoparticle surface plasmons, which are rapidly converted into electron–hole pairs (the rate constant of this process can be represented as B/R [22]; for Ag, e.g. one has $B \simeq 0.2$ eV nm [23]). From these perspectives, it seems that the use of nm-sized metal particles may be favourable. An additional factor in favour of such particles is that, in this case, the secondary electrons and holes are confined and do not migrate into the bulk. The former factor has already been widely discussed in the literature [22, 23]. For this reason, our discussion below is focused on the latter factor.

To illustrate the role of secondary electrons, it is instructive to treat the generic case when the primary electron and hole are generated due to the free-electron contribution to the absorbance, and their energy distribution is given by equation (2). To calculate the dependence of the SMPCP cross section on ω and E_0 (see equation (9)) for this case, we need expressions for the rate constants of energy relaxation of electrons and holes in nm-sized particles. As in the bulk case, this relaxation occurs primarily via electron–electron interaction, provided that the excitation energy is not too low. The available experimental data [24, 25] indicate that in nm-sized particles the electron energy relaxation due to electron–electron interaction may be faster than that in the bulk. On the other hand, the theoretical studies [26, 27] predict that the energy dependence of the rate constants characterizing electron–electron interactions is insensitive to the particle size. In particular, in analogy with equation (4), one can use [26]

$$r(E) = r_0[(E - E_F)/E_F]^2, \tag{10}$$

where r_0 is the energy-independent parameter.

In our calculations, we adopt expression (10), expression (2) for $f_0(E)$, and also expression (3) for the electron or hole energy distribution after the creation of a new electron–hole pair. The use of these expressions implies a large number of electronic states within a physically relevant energy range (for our discussion, this is about 0.1 eV). This assumption is expected to hold for metal particles with sizes about or above 1 nm. In addition, it is appropriate to note that

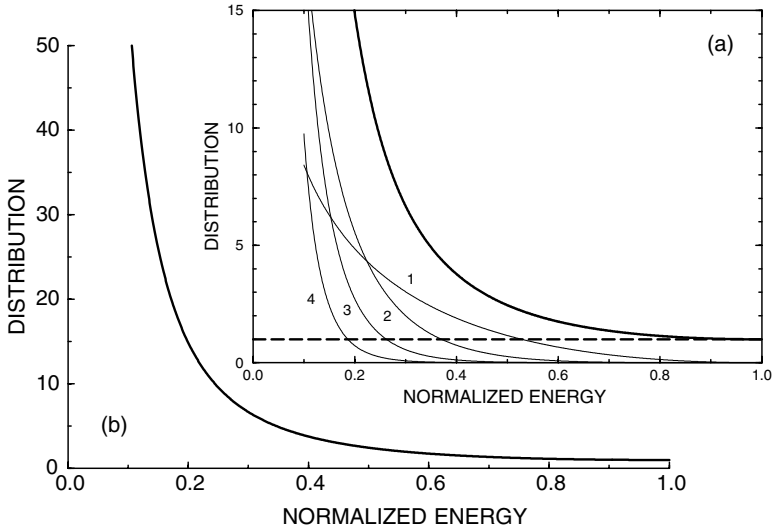

Figure 1. (a) Distribution of electrons as a function of the normalized energy, $(E - E_F)/(\hbar\omega)$, for the primary generation (dashed line), four secondary generations (thin solid lines), and the whole generation (thick solid line; equation (12) with $0 \leqslant i \leqslant 4$). Panel (b) shows the total distribution in more detail.

in reality nm-sized metal particles are located on a support or embedded in a host matrix and the relaxation of energy absorbed by such particles eventually occurs via the particle-support contacts. For hot electrons, however, the latter channel usually does not play a role.

Absorption of a photon results in the appearance of an excited electron and hole. After an act of energy relaxation of an electron, there will be one additional electron and one additional hole. A hole relaxes as well and hence there will also be one additional electron and one additional hole. Thus, after relaxation of the primary electron and hole, there are three excited electrons and three holes. Taking into account that the relaxation properties of the excited electrons and holes are similar, we have the following relationship between the electron distributions of two successive generations

$$f_{i+1}(E) = 3\int_E^{\hbar\omega} \varphi(\mathcal{E}, E)\, f_i(\mathcal{E})\, \mathrm{d}\mathcal{E}. \tag{11}$$

The total distribution is given by

$$f(E) = \sum_{i \geqslant 0} f_i(E). \tag{12}$$

With increasing i, the average electron energy rapidly decreases. Low-energy electrons ($E \leqslant \hbar\omega/10$) are however not of interest for our present treatment, because the reaction probability is negligible in this case (in addition, the energy relaxation of such electrons occurs via phonon excitation). For this reason, SMPCP can be described by taking into account only a few generations of secondary electrons. To illustrate the electron distributions, it is convenient to normalize the electron energy to $\hbar\omega$. With this normalization, the results of calculations become universal (see figure 1 showing the distribution of four generations of secondary electrons).

According to equation (9), the SMPCP cross section is proportional to $f(E_0)/r(E_0)$. Taking into account that $r(E) \propto (E - E_F)^2$ (equation (10)), it is instructive to introduce the

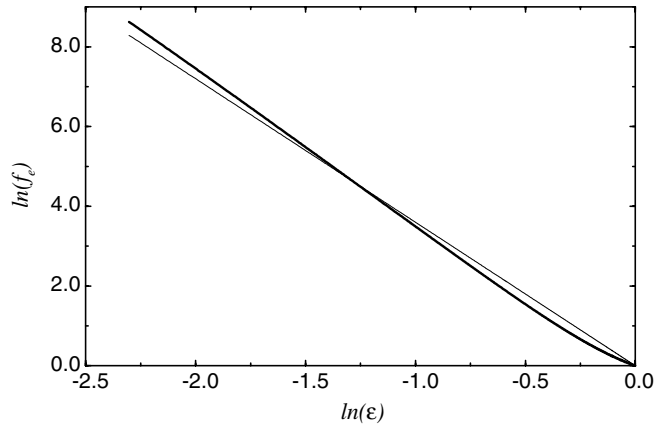

Figure 2. Logarithmic plot exhibiting the dependence of f_e on the normalized energy, $\epsilon \equiv (E_0 - E_F)/(\hbar\omega)$. The thick solid line was obtained by using equation (13) with $f(\epsilon)$ shown in figure 1(b). The thin solid line corresponds to equation (14).

dimensionless function

$$f_e(E_0) = f(E_0)(\hbar\omega)^3/(E_0 - E_F)^2, \tag{13}$$

which characterizes the dependence of the SMPCP cross-section on E_0. According to our calculations (figure 2), this function can be fitted as

$$f_e(E_0) = [\hbar\omega/(E_0 - E_F)]^{3.6}. \tag{14}$$

This expression explicitly shows that upon decreasing E_0 the contribution of secondary electrons to SMPCP on nm-sized particles very rapidly increases. For single-crystal surfaces, the corresponding dependence has not yet been accurately calculated (see the discussion above), but in the latter case the contribution of secondary electrons is not so significant.

3. Scenario 2

The second scenario of SMPCP implies the use of intensive sub-ps laser pulses of visible light [5]. In this case, the concentration of excited electrons and holes generated during a pulse near the surface is high. These electrons (or holes) may induce SMPCP as described in the previous section as long as their energy is appreciable. However according to the second scenario, the key role in SMPCP is prescribed to hot electrons (or holes) formed after a cascade of generation of secondary electron–hole pairs. The energy of these electrons is low compared to $\hbar\omega$ and also often relatively low compared to typical activation barriers for chemical processes. For this reason, a single hot electron (or hole) cannot induce SMPCP. Nevertheless, SMPCP are still possible due to multiple interaction (non-linear regime) of hot electrons with the adsorbate.

Due to high concentration and rapid mutual energy exchange, the hot electrons and holes are thermalized already during the laser pulse. The energy exchange with the lattice is, however, much slower. Under such conditions, the system can often be described by using the two-temperature model implying different electron and lattice (phonon) temperatures, T_e and T_l. This model, proposed in the mid-1970s [28], has been widely used and refined in different contexts [29, 30] including surface photochemistry [5]. For discussion of its limitations and more advanced approximations, one can read, e.g. [3, 31–34]. In general, the conditions

of applicability of the model depend on the material properties and optical excitation density. During a laser pulse, the electron interaction is obviously far from thermal at the very beginning (this stage corresponds more to scenario 1). The model may also fail at the late stages [34] presumably because the electron–electron interaction becomes weak. In photochemistry, one is interested in the stage when the electron temperature is close to maximum. This stage occurs for times comparable or slightly longer than the pulse duration. In this case, the predictions of the two-temperature model are often fairly reasonable (see e.g. experimental and theoretical data presented in figure 9 in [34]). For this reason, as noted in [5], the use of the two-temperature model makes sense. Employing the two-temperature model, one should verify that it is self-consistent. One of the simplest criteria is that the typical electron diffusion length should be larger that $1/\beta$ (see below).

In the available publications, applications of the two-temperature model are usually based on numerical calculations and do not allow one to easily compare and understand the specifics of different situations occurring in SMPCP. Our goal here is to articulate the model predictions directly relevant for SMPCP. Specifically, we derive simple analytical equations making it possible to classify various situations and to compare the efficiency of SMPCP on single-crystal surfaces and nm-sized particles.

In the framework of the second SMPCP scenario, the chemical process rate is not directly proportional to the photon flux. For this reason, instead of equations (1) and (8), one should rather operate with the SMPCP rate. In particular, the rate of SMPCP occurring on a single-crystal surface can be represented as

$$W(t) = k_{cp}(T_s(t))N_a(t), \tag{15}$$

where N_a is the number of adsorbed particles, $k_{cp}(T_s(t))$ the SMPCP rate constant, $T_s(t)$ the electron temperature near the surface, and t the time.

Excitation of adsorbate vibrations along the reaction coordinate occurs due to collisions with hot electrons, while relaxation of these vibrations is usually related to interaction with the lattice. Due to the difference between the electron and lattice temperatures, the dependence of k_{cp} on T_s is not reduced to the conventional Arrhenius expression with the activation energy equal to the barrier height (see generic discussion [5]). Nevertheless, this dependence is very strong, and accordingly the dominant contribution to the integral SMPCP rate results from the narrow temperature region near the temperature maximum. For this reason, we focus our attention below on the temperature behaviour near the maximum.

According to the two-temperature model, the equation for T_e is as follows:

$$C_e(T_e)\frac{\partial T_e}{\partial t} = \frac{\partial}{\partial z}\left(K_e(T_e)\frac{\partial T_e}{\partial z}\right) - G(T_e - T_l), \tag{16}$$

where $C_e(T_e) = A_e T_e$ and $K_e = K_0 T_e/T_l$ are the electron heat capacity and thermal conductivity (A_e and K_0 are constants), and G is the parameter characterizing the electron–phonon coupling. The typical electron diffusion length during the pulse duration is comparable to, or more often appreciably longer than $1/\alpha$. For this reason, we can consider that the absorbed heat, $I(t)$, is generated at $z = 0$ and use the corresponding boundary condition

$$K_e(T_e)\frac{\partial T_e}{\partial z}\bigg|_{z=0} = -I(t). \tag{17}$$

During and just after sub-ps heating, when the temperature is close to maximum, the second term in the right-hand (rh) part of equation (16) is negligible compared to the first term and can accordingly be dropped. In addition, the increase of the lattice temperature during this period is relatively small and one can use $K_e \simeq K_0 T_e/T_0$, where T_0 is the initial temperature.

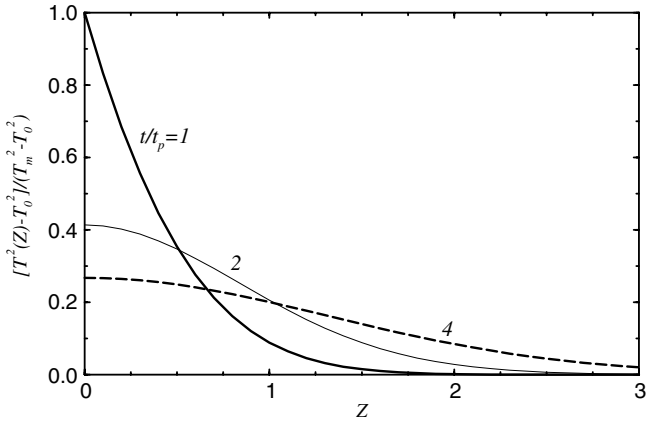

Figure 3. $[T_e^2(z,t) - T_0^2]/(T_m^2 - T_0^2)$ (equation (18)) as a function of the dimensionless coordinate, $Z \equiv z/(4\kappa t_p)^{1/2}$, for $t/t_p = 1$, 2 and 4.

Employing these approximations, assuming for simplicity the pulse to be rectangular, and using the standard Green-function technique, we can easily integrate equation (16) as

$$T_e^2(z,t) = T_0^2 + \frac{T_m^2 - T_0^2}{2t_p^{1/2}} \int_0^{t_*} \frac{\exp\{-z^2/[4\kappa(t-\tau)]\}}{(t-\tau)^{1/2}}\,\mathrm{d}\tau, \tag{18}$$

where T_m is the maximum electron temperature, t_p the pulse duration, $t_* = t$ for $t \leqslant t_p$ and $t_* = t_p$ for $t > t_p$, and $\kappa = K_0/(A_e T_0)$.

The SMPCP rate depends on $T_s(t)$ (note that $T_s(t) \equiv T_e(0,t)$). For this temperature, equation (18) yields

$$T_s^2(t) = T_0^2 + (T_m^2 - T_0^2)[t^{1/2} - (t-t_*)^{1/2}]/t_p^{1/2}. \tag{19}$$

For $t > t_p$, $t_* = t_p$ and accordingly

$$T_s^2(t) = T_0^2 + (T_m^2 - T_0^2)[t^{1/2} - (t-t_p)^{1/2}]/t_p^{1/2}. \tag{20}$$

If t is appreciably larger than t_p, the latter equation can be represented as

$$T_s^2(t) \simeq T_0^2 + (T_m^2 - T_0^2)(t_p/2t)^{1/2}. \tag{21}$$

To calculate the SMPCP yield, one should integrate the reaction rate (equation (15)) with the prescribed dependence of T_s on time. The results of this integration are however not universal, because the reaction rate (equation (15)) depends on various parameters characterizing a specific adsorbate–substrate system. For this reason, we prefer to focus our analysis on the derivation of simple criteria which make it possible to easily compare the length and time scales of heat propagation at $t > t_p$.

Figure 3 constructed by using equation (18) indicates that just after heating (at $t = t_p$) the typical electron diffusion length is given by

$$\langle z \rangle_h \simeq 1.5(\kappa t_p)^{1/2}. \tag{22}$$

This expression corresponds to $T(Z)/T_m \simeq 0.5$ (see the thick solid line in figure 3).

To characterize the drop of T_s at $t > t_p$, it is instructive to introduce the time $t_{3/4}$ corresponding to $T_s = (3/4)T_m$. According to equation (20), one has (provided that $T_s \gg T_0$)

$$t_{3/4} = 1.37t_p. \tag{23}$$

Table 1. Constants A_e, K_0 and G for Pt and Au, and the parameters characterizing the electron temperature behaviour near the Pt and Au flat surfaces and inside nm-sized particles in the case of laser pulses with $t_p = 200$ fs and $T_m = 4000$ K.

	Pt	Au	Units	Ref.
A_e	740	71	$\mathrm{J\,m^{-3}\,K^{-2}}$	[38]
K_0	73	318	$\mathrm{W\,m^{-1}\,K^{-1}}$	[38]
G	25×10^{16}	21×10^{15}	$\mathrm{W\,m^{-3}\,K^{-1}}$	[30]
$r_{1/2}$	0.54	0.48	–	Equation (24)
$\langle z\rangle_h$	12	82	nm	Equation (22)
$t_{3/4}$	270	270	fs	Equation (23)
$t_{3/4}$	3200	3600	fs	Equation (29)

In addition, it is of interest to estimate the ratio of the first and second terms on the right-hand side of equation (16) at $T_s = T_m/2$. The expression for the first term can be obtained by differentiating equation (21) with respect to time, multiplying the result by A_e, and taking into account that $T_s = T_m/2$ at $t \simeq 4t_p$ (see figure 3). Assuming also that $T_m \gg T_0$, we obtain the ratio of the two terms as

$$r_{1/2} = 32Gt_p/(A_eT_m). \tag{24}$$

Inside 1–10 nm-sized metal particles, it makes no sense to introduce gradients of electron temperature or concentration, because the size of such particles is smaller or comparable to $1/\beta$. This means that electrons in such particles can be described by using electron temperature which characterizes electrons in a whole particle. In other words, this means that in this limit equations (15) and (16) are not applicable and should be replaced by

$$W(t) = k_{cp}(T_e(t))N_a(t), \tag{25}$$

$$C_e(T_e)\,\mathrm{d}T_e/\mathrm{d}t = -G(T_e - T_l) + J(t), \tag{26}$$

where $J(t)$ is the energy absorbed per unit volume.

To solve equation (26), we again (i) take into account that, at electron temperatures near the maximum, heating of the lattice is nearly negligible ($T_l \simeq T_0$) and (ii) assume that the pulse is rectangular. In this case, we have

$$T_e(t) = [T_0^2 + (T_m^2 - T_0^2)t/t_p]^{1/2} \quad \text{at } t \leqslant t_p, \tag{27}$$

and

$$\left[T_m - T_e(t) + T_0 \ln\left(\frac{T_m - T_0}{T_e(t) - T_0}\right)\right] = \frac{G(t - t_p)}{A_e} \quad \text{at } t > t_p. \tag{28}$$

For $t_{3/4}$ [cf equation (23)], the latter equation yields (provided that $T_m \gg T_0$)

$$t_{3/4} \simeq t_p + A_eT_m/(4G). \tag{29}$$

To illustrate applications of the equations derived above, it is instructive to show what we may have in the case of sub-ps laser pulses on Pt and Au. The bulk properties of these two metals are quite different (table 1) and accordingly the range of the parameters characterizing the electron temperature behaviour near the Pt and Au flat surfaces and inside nm-sized particles is representative for many other metals as well. For example, we use $t_p = 200$ fs and $T_m = 4000$ K. In the case of a single-crystal surface (table 1), we have $r_{1/2} \simeq 0.5$ (this means that near the maximum temperature the role of the second term on the right-hand side of equation (16) is minor), $\langle z\rangle_h = 10$–80 (these values are comparable or appreciably larger

than $1/\alpha$), and $t_{3/4} = 270$ fs (see equation (23)). (Note that in the situations when $\langle z \rangle_h$ is comparable with $1/\alpha$ and accordingly with $1/\beta$ the applicability of equation (16) is limited. The applicability of equation (26) is limited in this case as well.)

For nm-sized particles, the constant G may be larger than that for the bulk due to excitation of acoustic or capillary surface vibrational modes [35]. The available experiments [36] indicate that for Au this constant is close to that for the bulk (while for Ag this does not seem to be the case). For this reason, to estimate $t_{3/4}$ for nm-sized Au and Pt particles, we employ the experimental bulk values of G [30] (one cannot exclude that these values should be somewhat higher [37], but it does not change qualitatively our conclusions). With these values, we obtain $t_{3/4} = 3200$–3600 fs. This means that in the case of nm-sized particles, the decrease of electron temperature after heating is about 10 times slower and accordingly due to this factor the efficiency of stimulation of SMPCP may be appreciably higher than that for single-crystal surfaces.

4. Conclusion

In summary, we have shown in detail that the confinement of electrons in nm-sized metal particles is beneficial for photochemistry both under low-intensity steady-state conditions and during intensive sub-ps laser pulses. Specifically, the confinement may increase the contribution of secondary hot electrons to the photochemical conversion. In the latter case, in addition, the decrease of electron temperature after heating may be much slower than that on single-crystal surfaces (see e.g. the results presented in table 1 for Au and Pt) and accordingly SMPCP may be more probable.

Finally, it is appropriate to notice that the equations and criteria, derived in our work, are simple and universal and accordingly can easily be employed to clarify various aspects of substrate-mediated photo-induced chemical processes occurring on single-crystal surfaces and supported nm-sized metal particles.

Acknowledgments

This work was supported by the Swedish Foundation for Strategic Research (Material Science project 'Multifunctional photoactive nanoparticles'). VPZ thanks E Hasselbrink for useful communication relating to [18, 20].

References

[1] Zhou X-L, Zhu X-Y and White J 1991 *Surf. Sci. Rep.* **13** 73
[2] Zimmermann F M and Ho W 1995 *Surf. Sci. Rep.* **22** 127
[3] Day H-L and Ho W (ed) 1995 *Laser Spectroscopy and Photochemistry on Metal Surfaces* (Singapore: World Scientific)
[4] Guo H, Saalfrank P and Seideman T 1999 *Prog. Surf. Sci.* **62** 239
[5] Gadzuk J W 2000 *Chem. Phys.* **251** 87
[6] Zhdanov V P and Kasemo B 1999 *Surf. Sci.* **432** L599
[7] Watanabe K, Matsumoto Y, Kampling M, Al-Shamery K and Freund H J 1999 *Angew. Chem. Int. Ed. Engl.* **38** 2328
[8] Kampling M, Al-Shamery K, Freund H-J, Wilde M, Fukutani K and Murata Y 2002 *Phys. Chem. Chem. Phys.* **4** 2629
[9] Wille A and Al-Shamery K 2003 *Surf. Sci.* **528** 230
[10] Kamat P V 2002 *J. Phys. Chem.* B **106** 7729
[11] Gunnarsson L, Bjerneld E J, Xu H, Petronis S, Kasemo B and Käll M 2001 *Appl. Phys. Lett.* **78** 802 and references therein

[12] Felidj N, Aubard J, Levi G, Krenn J R, Hohenau A, Schider G, Leitner A and Aussenegg F R 2003 *Appl. Phys. Lett.* **82** 3095
[13] Ritchie R H 1966 *J. Appl. Phys.* **37** 2276
[14] Snoke D W, Rühle W W, Lu Y-C and Bauser E 1992 *Phys. Rev.* B **45** 10979
[15] Echenique P M, Pitarke J M, Chulkov E V and Rubio A 2000 *Chem. Phys.* **251** 1
[16] Zhu X-Y, White J M, Wolf M, Hasselbrink E and Ertl G 1991 *Chem. Phys. Lett.* **176** 459
[17] Hellsing B, Chakarov D V, Osterlund L, Zhdanov V P and Kasemo B 1997 *J. Chem. Phys.* **106** 982
[18] Wie F, de Meijere A and Hasselbrink E 1993 *J. Chem. Phys.* **99** 682
[19] Hellsing B and Zhdanov V P 1994 *J. Photochem. Photobiol.* A **79** 221
[20] Harris S M, Holloway S and Hasselbrink E 1995 *Nucl. Instrum. Methods Phys. Res.* B **101** 31
[21] Vondrak T, Burke D J and Meech S R 2001 *Chem. Phys. Lett.* **347** 1
[22] Bertsch G F and Broglia R A 1994 *Oscillations in Finite Quantum Systems* (Cambridge: Cambridge University Press)
[23] Molina R A, Weinmann D and Jalbett R A 2002 *Phys. Rev.* B **65** 155427
[24] Voisin C, Christofilos D, Del Fatti N, Vallée F, Prevel B, Cottancin E, Lerme J, Pellarin M and Broyer M 2000 *Phys. Rev. Lett.* **85** 2200
[25] Del Fatti N and Vallée F 2001 *Appl. Phys.* B **73** 383
[26] Sivan U, Imry Y and Aronov A G 1994 *Europhys. Lett.* **28** 115
[27] Shahbazyan T V and Prakis I E 1999 *Phys. Rev.* B **60** 9090
[28] Anisimov S I, Kapelovich B L and Perel'man T L 1974 *Zh. Exp. Theor. Fiz.* **66** 776
[29] Kanavin A P, Smetanin I V, Isakov V A, Afanasiev Y V, Chichkov B N, Wellegehausen B, Nolte S, Momma C and Tunnermann A 1998 *Phys. Rev.* B **57** 14698
[30] Hohlfeld J, Wellershoff S-S, Güdde J, Conrad U, Jähnke V and Matthias E 2000 *Chem. Phys.* **251** 237
[31] Fann W S, Storz R, Tom H K M and Bokor J 1992 *Phys. Rev. Lett.* **68** 2834
[32] Groeneveld R H M, Sprik R and Lagendjik A 1995 *Phys. Rev.* B **51** 11433
[33] Grua P, Morreeuw J P, Bercegol H, Jonusauskas G and Vallée F 2003 *Phys. Rev.* B **68** 035424
[34] Lisowski M, Loukakos P A, Bovensiepen U, Stähler J, Gahl C and Wolf M 2004 *Appl. Phys. A: Mater. Sci. Proc.* **78** 165
[35] Fedorovich R D, Naumovets A G and Tomchuk P M 2000 *Phys. Rep.* **328** 73
[36] Hodak J H, Henglein A and Hartland G V 2000 *J. Phys. Chem.* B **104** 9954
[37] Hodak J H, Henglein A and Hartland G V 2001 *J. Chem. Phys.* **114** 2760
[38] Gray D E (ed) 1972 *American Institute of Physics Handbook* (New York: McGraw-Hill)